Published in final edited form as:
J Biomed Mater Res A. 2014 May ; 102(5): 1222–1230. doi:10.1002/jbm.a.35093.

Mesenchymal Stem Cell and Gelatin Microparticle Encapsulation in Thermally and Chemically Gelling Injectable Hydrogels for Tissue Engineering

Stephanie N. Tzouanas[1], **Adam K. Ekenseair**[1], **F. Kurtis Kasper**[1], and **Antonios G. Mikos**[1,*]
[1]Department of Bioengineering, Rice University, P.O. Box 1892, MS 142, Houston, TX 77251, USA

Abstract

In this work, we investigated the viability and osteogenic differentiation of mesenchymal stem cells encapsulated with gelatin microparticles (GMPs) in an injectable, chemically and thermally gelling hydrogel system combining poly(*N*-isopropylacrylamide)-based thermogelling macromers containing pendant epoxy rings with polyamidoamine-based hydrophilic and degradable diamine crosslinking macromers. Specifically, we studied how the parameters of GMP size and loading ratio affected the viability and differentiation of cells encapsulated within the hydrogel. We also examined the effects of cell and GMP co-encapsulation on hydrogel mineralization. Cells demonstrated long-term viability within the hydrogels, which was shown to depend on GMP size and loading ratio. In particular, increased interaction of cells and GMPs through greater available GMP surface area, use of an epoxy-based chemical gelation mechanism, and the tunable high water content of the thermogelled hydrogels led to favorable long-term cell viability. Compared to cellular hydrogels without GMPs, hydrogels co-encapsulating cells and GMPs demonstrated greater production of alkaline phosphatase by cells at all time-points and a transient early enhancement of hydrogel mineralization for larger GMPs at higher loading ratios. Such injectable, *in situ* forming hydrogels capable of delivering and maintaining populations of encapsulated mesenchymal stem cells and promoting mineralization *in vitro* offer promise as novel therapies for applications in tissue engineering and regenerative medicine.

Keywords

Cell encapsulation; Gelatin microparticles; Mineralization; Osteogenic differentiation; Thermogelling hydrogels

INTRODUCTION

Injectable *in situ* forming materials can address the challenges associated with craniofacial bone regeneration following trauma, tumor resection, or birth defects [1–3]. The high water content, minimally invasive delivery via injection, and cell and growth factor loading potential of hydrogels make them an exciting option in this regard. Thermogelling polymers are a promising candidate group as injectable hydrogels since they pass through a lower critical solution temperature (LCST) when injected into the body. Of note are poly(*N*-isopropylacrylamide) (PNiPAAm) hydrogels, given their tunability. Specifically, studies in the literature document control of the rate of thermally induced coil-globule phase transition,

*Corresponding Author: Professor Antonios G. Mikos, Department of Bioengineering, Rice University, P.O. Box 1892, MS 142, Houston, Texas, 77251-1892, USA. Tel.: +001-713-348-5355, Fax: +001-713-348-4244, mikos@rice.edu.

cell encapsulation potential, and *in vivo* performance of PNiPAAm [4–6]. At the same time, concerns regarding the propensity of injectable hydrogels to undergo syneresis must be taken into account [7].

Dual-hardening mechanisms that couple thermoresponsive properties with concurrent *in situ* crosslinking can begin to address the tendency of hydrogels to undergo syneresis [8]. Click chemistries and polymer pendant-group modification have been explored as options for the introduction of reactive double bonds but are limited by the need for cytotoxic initiators or catalysts to allow for crosslinking [9]. Methacrylate and acrylate-modified macromers of PNiPAAm also present cytotoxicity concerns, underscoring the need for a crosslinking reaction of short duration [6]. Furthermore, once formed, PNiPAAm-based dual-hardening hydrogels often do not degrade at a physiologically relevant rate [10]. The slow timescale of degradation of PNiPAAm-based dual-hardening hydrogels points to the need for modifications to promote network degradation.

Towards this end, systems combining two macromers offer several advantages. Especially important is the ability to adjust hydrogel properties, such as degree of crosslinking, at the hydrogel formulation phase instead of the macromer synthesis phase. Additionally, cytocompatible and degradable crosslinkers allow for separation of control of the degradation and thermoresponsive properties to different system components. Injectable, water-soluble polymers, such as polyamidoamines (PAMAMs), are a compelling choice for inclusion in two-component systems. Biocompatible and easy to synthesize, PAMAMs can be synthesized to have a linear structure with amine or acrylamide ends [11]. The degradation rate of PAMAM can be tuned through the inclusion of higher-functionality crosslinkers, additional reactive pendant moieties, and comonomers such as bisacrylamides and diamines [12, 13].

Previous work by this group has developed a thermogelling macromer based on PNiPAAm with pendant epoxy rings and a degradable PAMAM crosslinker for dual-hardening, injectable, and hydrolytically degradable hydrogels [13]. The system's hydrophilicity due to PAMAM incorporation has been shown to eliminate syneresis upon formation in a fully tunable fashion [13]. Moreover, epoxy-based crosslinking enabled quick PAMAM incorporation into the polymer network throughout and after thermogellation. Cytocompatibility of all components of the system, including the PNiPAAm macromer, PAMAM crosslinker, formed hydrogel leachables, and hydrogel degradation products, has been demonstrated at the concentrations of interest [14].

The goal of this study was to explore the loading potential of this system with respect to cells and the effects of co-encapsulation of gelatin microparticles (GMPs). The delivery of mesenchymal stem cells (MSCs) through the hydrogel system can assist in the regenerative process by providing important signaling activities and promoting healing in the defect region. MSCs can modulate the local immune and inflammatory response of the host, differentiate into bone-forming cells, enhance the rate of tissue regeneration of bone-forming cells, and facilitate matrix deposition [15]. While gelatin microparticles have been incorporated into hydrogel systems as a means of offering a controlled release system for growth factors, gelatin microparticles can also serve as enhancers of calcium deposition [16]. The effects of co-loading the PNiPAAm macromer and PAMAM crosslinker hydrogel system with MSCs and GMPs was studied with respect to cell survival, osteogenic differentiation, and mineralization. The objectives of this study were to assess the viability of cells encapsulated within the hydrogel with and without GMP co-encapsulation, to investigate the effects of GMP size and loading ratio on MSC cell survival and differentiation, and to examine the effects of GMP and MSC encapsulation on hydrogel mineralization.

MATERIALS AND METHODS

Experimental design

A factorial study design was implemented to study the effects of GMP size, GMP loading ratio, and cellularity on cell viability, cell differentiation, and hydrogel mineralization [Table 1]. Two GMP size ranges, 50–100 μm and 250–300 μm, were considered. GMP loading ratio was designated as the ratio between GMP and dry hydrogel mass, and two loading ratios, 1:20 and 1:5, were studied. Five groups of cellular hydrogels were evaluated (No GMPs, 1:20 loading of 50–100 μm GMPs, 1:5 loading of 50–100 μm GMPs, 1:20 loading of 250–300 μm GMPs, and 1:5 loading of 250–300 μm GMPs). The same five GMP size and loading conditions were studied in acellular hydrogels as well. Time-points were taken after 0, 7, 14, 21, and 28 days.

Materials

N-Isopropylacrylamide (NiPAAm), glycidyl methacrylate (GMA), 2,2′-azobis(2-methylpropionitrile) (azobisisobutyronitrile, AIBN), *N*,*N*′-methylenebisacrylamide (MBA), and piperazine (PiP) were purchased from Sigma-Aldrich (Sigma, St. Louis, MO) and used as received. The solvents−tetrahydrofuran (THF), dimethylformamide (DMF), diethyl ether, and acetone in analytical grade and water, acetonitrile, chloroform, and methanol in HPLC grade–were obtained from VWR (Radnor, PA) and used as received. Phosphate buffered saline (PBS) solution was mixed from powder (pH 7.4, Gibco Life, Grand Island, NY), and ultrapure water was obtained from a Millipore Super-Q water system (Millipore, Billerica, MA).

Thermogelling macromer (TGM) synthesis

The thermogelling macromer poly(NiPAAm-*co*-GMA) was synthesized by free radical polymerization as previously described [13]. Ten g of the comonomers, NiPAAm and GMA, at 92.5 and 7.5 mol %, respectively, was dissolved in 100 mL of DMF and polymerized at 65 °C under a nitrogen atmosphere. AIBN was added as a free radical initiator at 0.7 mol % of the total monomer content, and the reaction mixture was continuously stirred for 20 h. The product was concentrated by rotary evaporation, dissolved in a 95:5 (v/v) mixture of acetone and methanol, and twice precipitated in at least 10 times excess of cold diethyl ether to remove effectively the unreacted monomers and low-molecular-weight oligomers. The final filtrate was dried under vacuum at ambient temperature to yield a fine white powder.

PAMAM synthesis

As previously described [13], the polyamidoamine (PAMAM) crosslinking macromer was synthesized by polyaddition of piperazine (PiP) with *N*,*N*′-methylenebisacrylamide (MBA). 10.83 g of the comonomers was dissolved in 30 mL of ddH_2O with a stoichiometric excess of PiP (r = [MBA]/[PiP] = 0.78), stirred continuously under nitrogen atmosphere at 30 °C, and allowed to react for 48 h according to published procedures [13]. The obtained viscous mixture was directly precipitated in 100 mL of acetone, filtered, and dried under vacuum at ambient temperature to yield a fine powder. The PAMAM was found to have a M_n of 1960, M_w of 2380, and PDI of 1.22 by means of microTOF ESI mass spectroscopy (data not shown), which is consistent with previous investigations [13, 14].

GMP synthesis and pre-swelling

Gelatin microparticles were synthesized using a procedure adapted from published protocols [17]. Five g of acidic gelatin with an isoelectric point of 5.0 (Nitta Gelatin Corporation, Osaka, Japan) was dissolved into 45 mL ddH_2O to achieve 50 to 100 μm diameter particles while 7.5 g gelatin was dissolved into 40 mL ddH_2O to achieve 250 to 300 μm diameter

particles. Dissolution was achieved by means of stirring the solution intermittently while keeping it at 70 °C. The resulting solution was added dropwise to a mixture of 250 mL olive oil and 1.25 mL Span 80, which was mixed at 500 rpm using an overhead stirrer. The reaction vessel was surrounded by ice and the emulsion was allowed to continue to mix for 30 min, at which point 100 mL of chilled acetone was added dropwise to the emulsion. After an additional 1 h of mixing, the formed microparticles were filtered out and washed with acetone. Crosslinking of the microparticles with 10 mM glutaraldehyde was achieved by incubating them in a solution of 0.5 mL Tween 80 in 500 mL ddH_2O with 1 g glutaraldehyde while stirring at 500 rpm and keeping the reaction vessel surrounded by ice. The crosslinking reaction was terminated after 20 h by adding 0.9375 g glycine to the reaction vessel and allowing the mixture to stir for 1 h. The crosslinked microparticles were isolated by filtering and washing with chilled water and acetone. Microparticles were then stored in a −80 °C freezer for 1 h before being lyophilized overnight. The next day, particles were sieved to collect those with diameters between 50 and 100 μm and between 250 and 300 μm. Morphology and size of GMPs for a given distribution were confirmed using Scanning Electron Microscopy (FEI Quanta 400 Environmental, Hillsboro, OR) (data not shown). Prior to imaging, GMPs were placed on an adhesive SEM stage and sputter-coated with gold. In order to prepare GMPs for incorporation into the hydrogel itself, the GMPs were pre-swollen in PBS in a 5 mL PBS to 1 g GMP ratio for 16 h.

Rat MSC isolation and preculture

MSCs were harvested from marrow from the femora and tibiae of male 6–8-week-old Fischer 344 rats (Charles River Laboratories, Wilmington, MA) as previously described [18]. The procedures followed were approved by the Institutional Animal Care and Use Committee of Rice University. MSCs were then cultured on T-75 flasks in Eagle-α modified minimum essential medium (Sigma, St. Louis, MO) supplemented with 10 vol.% fetal bovine serum (FBS) (Cambrex BioScience, Charles City, IA), 10 mM β-glycerol 2-phosphate, 50 μg/mL ascorbic acid, 50 μg/mL gentamicin, 100 μg/mL ampicillin and 1.25 μg/mL fungizone (Sigma, St. Louis, MO). Cells were cultured in a humidified incubator at 37 °C and 5% CO_2. Medium was changed after 24 h to remove non-adherent cells and every 2 days thereafter until confluence was reached. MSCs were then lifted with 0.25% trypsin/EDTA (Gibco), counted using a hemocytometer, centrifuged and resuspended into osteogenic medium (the aforementioned medium supplemented with 0.01 μM dexamethasone) at a concentration of 24×10^6 cells/mL for encapsulation into hydrogels.

Cell encapsulation and culture

Vacuum-dried TGM and PAMAM macromers were sterilized by UV exposure for 2 h prior to hydrogel preparation. As previously described [13], individual solutions of the TGM and PAMAM macromers in PBS were prepared at twice the desired final solution concentrations. The hydrogels were formulated to contain 15 wt % TGM and PAMAM was added at a 1:1 mol ratio between amine end groups and pendant epoxy rings in the TGM in order to achieve the maximum theoretical degree of crosslinking. After 20 min at 4 °C, 110 μL injections were made into 37 °C Teflon molds (8 mm in diameter and 2 mm in height) using cold pipet tips, and the hydrogels were allowed to gel chemically and thermally for 1 h.

Incorporation of GMPs into the hydrogel system was accomplished by adding the preswollen GMPs directly into the mixture of TGM and PAMAM solutions. Incorporation of MSCs into the hydrogel system required that PAMAM was dissolved into 250 μL PBS at four times the desired concentration in order to ensure that TGM and PAMAM concentrations were the same for hydrogels encapsulated with cells. MSCs were suspended in 250 μL of osteogenic medium at a concentration of 24×10^6 cells/mL. The cell suspension

was mixed gently into the TGM and PAMAM solution mixture just before injection into the molds. After 1 h, the formed hydrogels were removed from the molds and transferred to individual wells of a 12-well plate and immersed in 2.5 mL of osteogenic medium and kept in the incubator for either 0, 7, 14, 21, or 28 days (n=4). Medium was changed every 2–3 days. Acellular groups with a 1:5 or 1:20 GMP loading (by dry weight of polymer) of 50–100 μm and 250–300 μm diameter particles and a cellular group without GMP loading served as the controls.

Biochemical assays

Hydrogels from each group were collected for analysis after 0, 7, 14, 21, and 28 days of incubation (n = 4). Hydrogels were cut in half, with four halves designated for biochemical assays, two halves for confocal fluorescence microscopy, and two halves for histological imaging. Each of the four hydrogel halves reserved for assays was submerged in 500 μL ddH_2O and then broken up using an 18 ½ gauge needle to repeatedly draw up and release the mixture. Further homogenization was achieved by means of three consecutive freeze/thaw/sonication cycles (10 min at −80°C, 10 min at 37°C, 10 min sonication). As described in the literature, the viability of the MSCs encapsulated in the hydrogel was assessed by means of a Quant-iT Picogreen DNA assay (Molecular Probes, Eugene, OR) [10]. The values obtained from the DNA assay were normalized to the hydrogel weight including encapsulated cells and GMPs, and the values from acellular sample groups were subtracted off of their corresponding cellular sample groups. Providing an indication of the system's inherent mineralization properties and the osteogenic differentiation of the encapsulated MSCs, mineralization was assessed by means of a Genzyme calcium assay (Genzyme Diagnostics PEI, Charlottetown, Prince Edward Island, Canada). The values obtained from the calcium assay were normalized to the hydrogel weight. Alkaline phosphatase (ALP), an early marker of osteogenic differentiation, was measured using the Sigma-Aldrich ALP assay (Sigma, St. Louis, MO). For each condition, values from acellular sample groups were subtracted from the values of their corresponding cellular sample groups, which were then normalized to the difference between values of cellular and acellular groups obtained from the DNA assay.

Confocal fluorescence microscopy

Transverse hydrogel sections of 0.5–1 mm thickness were incubated with 2 μM calcein AM and 4 μM ethidium homodimer-1 per the manufacturer's instructions (Live/Dead Viability/Cytotoxicity Kit, Invitrogen, Eugene, OR). Cellular viability and distribution were evaluated with a confocal fluorescence microscope (LSM 510 META, Carl Zeiss, Germany) using a 10× objective. Argon and helium–neon lasers were used for excitation at 488 and 543 nm, respectively, and emission filters at 505–526 and 612–644 nm were employed.

Histology

Hydrogels were embedded in freezing medium (Histo-Prep, Fisher Scientific, Fair Lawn, NJ) and frozen at −20 °C. Frozen longitudinal sections of 5 μm thickness were cut with a cryostat (Leica CM3050S, Bannockburn, IL). Sections were stained with von Kossa reagent according to published protocols [10]. Samples were immersed in 1% silver nitrate solution (Sigma) under UV for 30 min to visualize phosphate, an important component of bone mineralization. Sections were imaged with a light microscope and camera (LSM 510 META, Carl Zeiss, Germany).

Statistics

The data are expressed as means ± standard deviation for four replicates. Statistically significant differences were determined by Tukey's post hoc test ($p < 0.05$) within time

points. Analysis of the main effects and parameter interactions in the 2^2 and 2^3 full factorial experimental designs was completed according to published methods [19].

RESULTS

Encapsulated cell viability in GMP-loaded hydrogels

Cells remained viable within the hydrogels 28 days after encapsulation [Fig. 1A]. Hydrogels were prepared from a cell suspension with an initial seeding density of 24 million cells/mL. However, a decrease in cell viability was observed in all groups between the Day 0 time-point and subsequent time-points. Compared to MSCs encapsulated without GMPs, MSC viability decreased when co-encapsulated with GMP regardless of particle size and loading. However, MSCs co-encapsulated with 50–100 μm GMPs remained more viable across time-points than MSCs co-encapsulated with 250–300 μm GMPs. These findings were confirmed using confocal microscopy to view Live/Dead-stained hydrogel sections [Fig. 1B]. Significant quantities of live cells were visible across all groups and time-points.

To better understand the effects and interactions of GMP loading and GMP size on cell viability, a factorial experimental analysis with low and high values of each parameter was employed. Analysis was carried out per established protocols [19], and results for the DNA assay are shown in Fig. 2, which details the magnitude of the main effects of each variable as well as the interactions between the variables. All effects associated with each variable and variable-pair interaction are shown with error bars signifying the standard error of each effect population.

The most significant effect with respect to MSC viability was GMP size. Up to and including the Day 21 time-point, increasing GMP size resulted in diminished cell viability [Fig. 2]. For all time-points, cell viability was improved in hydrogels with higher GMP loading compared to those with lower GMP loading [Fig. 2]. To better understand the interplay between GMP loading and GMP size, the cross effects of these two factors were studied (data not shown). At the Day 14 and 21 time-points, factorial analysis showed that there was a synergistic interaction between decreasing GMP loading and decreasing GMP size, which led to enhanced cell viability. Thus, at the lower GMP loading ratio, a greater increase in cell viability was observed for a reduction in particle size.

ALP activity of MSCs encapsulated in GMP-loaded hydrogels

MSCs encapsulated without GMPs demonstrated a peak in ALP expression at the Day 21 time-point [Fig. 3], indicating progress down the osteogenic pathway [20]. In all groups loaded with GMPs, ALP expression increased over time. MSCs co-encapsulated with 250–300 μm GMPs exhibited more pronounced ALP expression compared to those co-encapsulated with 50–100 μm GMPs. MSCs co-encapsulated with small GMPs displayed levels of ALP expression at the Day 28 time-point that were higher than those at earlier time-points. MSCs co-encapsulated with large GMPs in the 1:5 ratio also had levels of ALP expression at the Day 28 time-point that were higher than those at earlier time-points. However, MSCs co-encapsulated with large GMPs in the 1:5 ratio did not exhibit differences in levels of ALP expression between time-points after Day 0.

Calcium deposition in acellular and cellular GMP-loaded hydrogels

All groups demonstrated an increase in calcium present from initial levels at the Day 0 time-point [Fig. 4]. Hydrogels loaded with only GMPs exhibited increases between the Day 7 and Day 28 time-points as well. Hydrogels loaded with both MSCs and GMPs did not exhibit differences in calcium levels between the Day 7 and Day 28 time-points. Cellular hydrogels loaded with GMPs 250–300 μm in diameter presented peaks in the levels of calcium present

at the Day 21 time-point. These results were confirmed through von Kossa histological staining [Fig. 5].

Factorial experimental analysis revealed that the significant effects influencing calcium deposition in the cellular and acellular hydrogels changed over time. Hydrogels at earlier time-points, such as the Day 14 time-point shown in Fig. 6, exhibited increased mineralization when GMP loading (factor A) and GMP size (factor C) were increased and when MSCs (factor B) were not encapsulated within the hydrogel. However, hydrogels at the Day 21 time-point presented increased mineralization when MSCs (factor B) and when larger GMPs (factor C) were encapsulated in the hydrogels [Fig. 6]. By Day 28, the only main effect with significant influence on calcium deposition was the cellularity of the hydrogel (factor B) [Fig. 6]. Factorial analysis indicated that the absence of MSCs (factor B) at the Day 28 time-point improved calcium deposition.

The cross effects of significant interactions between GMP loading, hydrogel cellularity, and GMP size were considered for the Day 14 and Day 21 time-points to better understand their impact on calcium deposition within the hydrogel [Fig. 7]. Increasing GMP size is shown to cause significant increases in early mineralization only at a lower GMP loading ratio (AC Interaction). Beyond 14 days, this interaction is no longer evident. The effect of increasing GMP size was also confounded by the co-encapsulation of cells within the hydrogels, which is represented by the BC interaction. At the Day 14 time-point, acellular groups exhibited greater mineralization with larger particle size, while cellular groups displayed the opposite trend. At the Day 21 time-point, the interaction was the reverse, and at the Day 28 time-point, the interaction was no longer evident. Finally, for only the Day 21 time-point, increasing GMP loading for cellular hydrogels resulted in an increase in mineralization, while increasing GMP loading for acellular hydrogels resulted in a decrease in mineralization (AB interaction).

DISCUSSION

The objectives of this study were to assess the viability of cells encapsulated within the hydrogel with and without GMP co-encapsulation, to investigate the effects of GMP size and loading ratio on MSC differentiation, and to examine the effects of GMP and MSC encapsulation on hydrogel mineralization. The hydrogel system combined poly(*N*-isopropylacrylamide)-based thermogelling macromers containing pendant epoxy rings with polyamidoamine-based hydrophilic and degradable diamine crosslinking macromers and formed through thermal and chemical gelation. GMPs have been used extensively in previous drug delivery efforts to promote tissue regeneration in bone defects and demonstrate an inherent tendency to accrue mineralization [16]. While GMPs are commonly loaded with growth factors and other biomolecules of interest, it is important to bear in mind the effects that GMPs have on the hydrogel itself as well as the MSCs encapsulated within the system.

Cells remained viable across all time-points when encapsulated within the hydrogel, which underscores the potential of the hydrogel system for cell delivery applications. However, viability was decreased when MSCs were co-encapsulated with GMPs. All cellular hydrogels were loaded in the same cell per hydrogel volume ratio, and for hydrogels loaded with both MSCs and GMPs, less hydrogel volume was available to the cells. Furthermore, higher GMP loading resulted in decreased cell viability across the board, even at the Day 0 time-point. This suggests that the alteration of hydrogel solution mixing and injection procedures to incorporate GMPs negatively affected initial cell survival. However, MSCs co-encapsulated with smaller GMPs, i.e. 50–100 μm diameter, were more viable over time compared to MSCs co-encapsulated with larger GMPs, i.e. 250–300 μm diameter. At the

same total volume content of GMPs, smaller particles offer greater available surface area and consequently lead to enhanced interaction between GMPs and the surrounding cells and hydrogel. After all, MSCs are anchorage dependent cells [21], and GMPs provide an attachment site for MSCs encapsulated within the hydrogel. Thus, the interaction between the co-encapsulated cells and gelatin microparticles was beneficial for long-term cell viability [16].

MSCs co-encapsulated with GMPs into the hydrogel system also demonstrated altered ALP expression patterns. Typically, MSCs cultured in osteogenic medium exhibit a peak in ALP expression as they differentiate down the osteogenic pathway [15]. The ALP expression pattern displayed by the cellular hydrogel group without GMPs was consistent with this trend; the highest levels of ALP expression occurred at the Day 21 time-point. MSCs co-encapsulated with GMPs demonstrated enhanced and continually increasing rates of ALP expression over 28 days. This increase in ALP expression may reflect a positive effect of cell-GMP interaction as seen with cell survival. At the same time, the conditions with poorer cell survival, i.e. less cell-GMP interaction area, had better outcomes with respect to ALP expression. This finding is consistent with the fact that MSCs tend to differentiate when round rather than when attached to a surface [21].

Studying the effects of GMP encapsulation on the mineralization of hydrogels also yielded important insights. Through factorial analysis, GMP size was found to be a significant main effect in influencing calcium deposition for all time-points excluding the Day 28 time-point, especially at the higher loading ratio. Specifically, increasing GMP size led to increased calcium deposition. On the other hand, smaller GMPs offer greater surface area for interaction with MSCs, which was observed to promote cell survival. This could reveal a trade-off between cell survival and calcium deposition. With this in mind, cellularity was a significant main effect with respect to calcium deposition, leading to reduced hydrogel mineralization across all time-points, with the notable exception of the large GMP groups at the Day 21 time-point.

These observations may be better understood in light of the findings gleaned from the von Kossa histological staining performed [Fig. 5]. Histological staining suggests that for the cellular hydrogels, GMPs had begun undergoing degradation over the course of the study. Findings in the literature indicate that MSCs can promote the degradation of GMPs through the secretion of matrix metalloproteinases [22]. With this in mind, the peak in calcium for the hydrogels co-encapsulating MSCs and GMPs at the Day 21 time-point may reflect the release of calcium accrued within the larger volume of the particles due to degradation of the GMPs induced by MSC-secreted factors. The isoelectric point of the GMPs is 5.0, which explains their mineralization at a physiological pH of 7.4 given their negative charge. The marked release of calcium from the larger GMPs can be rationalized in light of the greater reservoir volume available. The possible degradation of GMPs over time can also explain the lack of significant main effects observed for the variables of GMP loading and GMP size at the Day 28 time-point.

Aside from GMP degradation, it is important to consider other factors influencing hydrogel mineralization. The hydrogel system studied possesses an innate ability to mineralize due to the hydrophobicity of the TGM above its LCST. However, degradation of GMPs can affect the condition of and promote degradation of the hydrogel itself. Additionally, calcium present can also be attributed to deposition by MSCs. The mineralization trends observed likely reflect cross-talk between cell differentiation, hydrogel condition, and GMP degradation. In summation, the encapsulation of GMPs within the hydrogel facilitated mineralization at earlier time-points but did not augment the hydrogel's final mineralization potential possibly due to degradation over the timescale studied.

CONCLUSIONS

The effects of GMP size and loading ratio on the viability, ALP expression, and calcium deposition of MSCs encapsulated within *in situ* dual-gelling injectable hydrogels that combine PNiPAAm-based TGMs and PAMAM-based crosslinking macromers were studied. Cells demonstrated long-term viability within the hydrogels, and MSC viability was shown to depend on GMP size, with smaller GMPs at higher loading ratios allowing for better viability outcomes, likely due to increased surface area for interaction and attachment. Greater interaction between GMPs and MSCs through higher GMP surface area further resulted in lower levels of ALP expression and hydrogel mineralization, which can be attributed to enhanced MSC differentiation in a suspended rather than attached state.

The hydrogel system considered, both with and without the co-encapsulation of GMPs, was shown to be suitable for MSC encapsulation and survival for a period up to and including 28 days. Both the epoxy-based chemical gelation pathway, which is rapid, requires no cytotoxic initiator or catalyst molecules, and leaves no residue post-reaction, and the enhanced hydrogel water content through incorporation of PAMAM provided favorable long-term cell viability. Calcium deposition in the hydrogels was enhanced at earlier time-points when GMPs were encapsulated within the system, particularly for larger GMPs presenting greater available reservoir volume. While the long-term mineralization potential of the hydrogels was reduced by encapsulation of MSCs, hydrogel mineralization was unaffected by GMP loading at the conditions considered. Thus, the injectable, dual-gelling hydrogel scaffold studied holds promise and merits further investigation for application as a cell delivery component of novel therapies in tissue engineering and regenerative medicine.

Acknowledgments

This work was supported by a grant from the National Institutes of Health (R01 DE17441). Tiffany Vo is acknowledged for her comments and suggestions regarding the manuscript.

REFERENCES

1. Gutowska A, Jeong B. Injectable gels for tissue engineering. M. Anat. Rec. 2001; 263:342–349.
2. Ekenseair AK, Kasper FK, Mikos AG. Perspectives on the interface of drug delivery and tissue engineering. Adv. Drug Deliv. Rev. 2013; 65(1):89–92. [PubMed: 23000743]
3. Vo TN, Kasper FK, Mikos AG. Strategies for controlled delivery of growth factors and cells for bone regeneration. Adv. Drug Deliv. Rev. 2012; 64(12):1292–1309. [PubMed: 22342771]
4. Emik S, Gurday GJ. Synthesis and swelling behavior of thermosensitive poly(*N*-isopropyl acrylamide-co-sodium-2-acrylamido-2-methyl propane sulfonate) and poly(*N*-isopropyl acrylamide-co-sodium-2-acrylamido-2-methyl propane sulfonate-co-glycidyl methacrylate) hydrogels. Appl. Polym. Sci. 2006; 100:428–438.
5. Guan JJ, Hong Y, Ma ZW, Wagner WR. Protein-reactive, thermoresponsive copolymers with high flexibility and biodegradability. Biomacromolecules. 2010; 11:1873–1881. [PubMed: 20575552]
6. Klouda L, Hacker MC, Kretlow JD, Mikos AG. Cytocompatibility evaluation of amphiphilic, thermally responsive and chemically crosslinkable macromers for in situ forming hydrogels. Biomaterials. 2009; 30:4558–4566. [PubMed: 19515420]
7. Hacker MC, Klouda L, Ma BB, Kretlow JD, Mikos AG. Synthesis and Characterization of Injectable, Thermally and Chemically Gelable, Amphiphilic Poly(*N*-isopropylacrylamide)-Based Macromers. Biomacromolecules. 2008; 9:1558–1570. [PubMed: 18481893]
8. Robb SA, Lee BH, McLemore R, Vernon BL. Simultaneously Physically and Chemically Gelling Polymer System Utilizing a Poly(NIPAAm-co-cysteamine)-Based Copolymer. Biomacromolecules. 2007; 8:2294–2300. [PubMed: 17567067]

9. Wang ZC, Xu XD, Chen CS, Yun L, Song JC, Zhang XZ, Zhao RX. In Situ Formation of Thermosensitive PNiPAAm-Based Hydrogels by Michael-Type Addition Reaction. ACS Appl. Mater. Interfaces. 2010; 2:1009–1018. [PubMed: 20423120]
10. Klouda L, Perkins KR, Watson BM, Hacker MC, Bryant SG, Raphael RM, Kasper FK, Mikos AG. Thermoresponsive, in situ cross-linkable hydrogels based on *N*-isopropylacrylamide: Fabrication, characterization and mesenchymal stem cell encapsulation. Acta Biomater. 2011; 7:1460–1467. [PubMed: 21187170]
11. Dey RK, Ray AR. Synthesis, characterization and blood compatibility of copolymers derived from polyamidoamines and vinyl acetate. J. Macromol. Sci., Part A: Pure Appl. Chem. 2005; A42:351–364.
12. Ferruti P, Marchisio MA, Duncan R. Poly(amido-amine)s: Biomedical Applications. Macromol. Rapid Commun. 2002; 23:332–355.
13. Ekenseair AE, Boere KWM, Tzouanas SN, Vo TN, Kasper FK, Mikos AG. Synthesis and Characterization of Thermally and Chemically Gelling Injectable Hydrogels for Tissue Engineering. Biomacromolecules. 2012; 13:2821–2830. [PubMed: 22881074]
14. Ekenseair AE, Boere KWM, Tzouanas SN, Vo TN, Kasper FK, Mikos AG. Structure-Property Evaluation of Thermally and Chemically Gelling Injectable Hydrogels for Tissue Engineering. Biomacromolecules. 2012; 13:1908–1915. [PubMed: 22554407]
15. Jaiswal N, Haynesworth SE, Caplan AI, Bruder SPJ. Osteogenic differentiation of purified, culture-expanded human mesenchymal stem cells in vitro. Cell Biochem. 1997; 64:295–312.
16. Hayashi K, Tabata Y. Preparation of stem cell aggregates with gelatin microspheres to enhance biological functions. Acta Biomater. 2001; (7):2797–2803.
17. Holland TA, Tabata Y, Mikos AG. In vitro release of transforming growth factor-β1 from gelatin microparticles encapsulated in biodegradable, injectable oligo(poly(ethylene glycol) fumarate) hydrogels. J. Control Release. 2003; 91(3):299–313. [PubMed: 12932709]
18. Datta N, Holtorf HL, Sikavitsas VI, Jansen JA, Mikos AG. Effect of bone extracellular matrix synthesized in vitro on the osteoblastic differentiation of marrow stromal cells. Biomaterials. 2005; 26(9):971–977. [PubMed: 15369685]
19. Montgomery, DC. Design and Analysis of Experiments. 3rd ed. New York: John Wiley & Sons; 1991.
20. Shin H, Temenoff JS, Bowden GC, Zygourakis K, Farach-Carson MC, Yaszemski MJ, Mikos AG. Osteogenic differentiation of rat bone marrow stromal cells cultured on Arg-Gly-Asp modified hydrogels without dexamethasone and β-glycerol phosphate. Biomaterials. 2005; 26(17):3645–3654. [PubMed: 15621255]
21. Shin H, Seongbong Jo, Mikos AG. Modulation of marrow stromal osteoblast adhesion on biomimetic oligo[poly(ethylene glycol) fumarate] hydrogels modified with Arg-Gly-Asp peptides and a poly(ethylene glycol) space. J. Biomed. Mater. Res. 2002; 61(2):169–179. [PubMed: 12061329]
22. Patel ZS, Yanamoto M, Ueda, Tabata Y, Mikos AG. Biodegradable gelatin microparticles as delivery systems for the controlled release of bone morphogenetic protein-2. Acta Biomater. 2008; 4(5):1126–1138. [PubMed: 18474452]

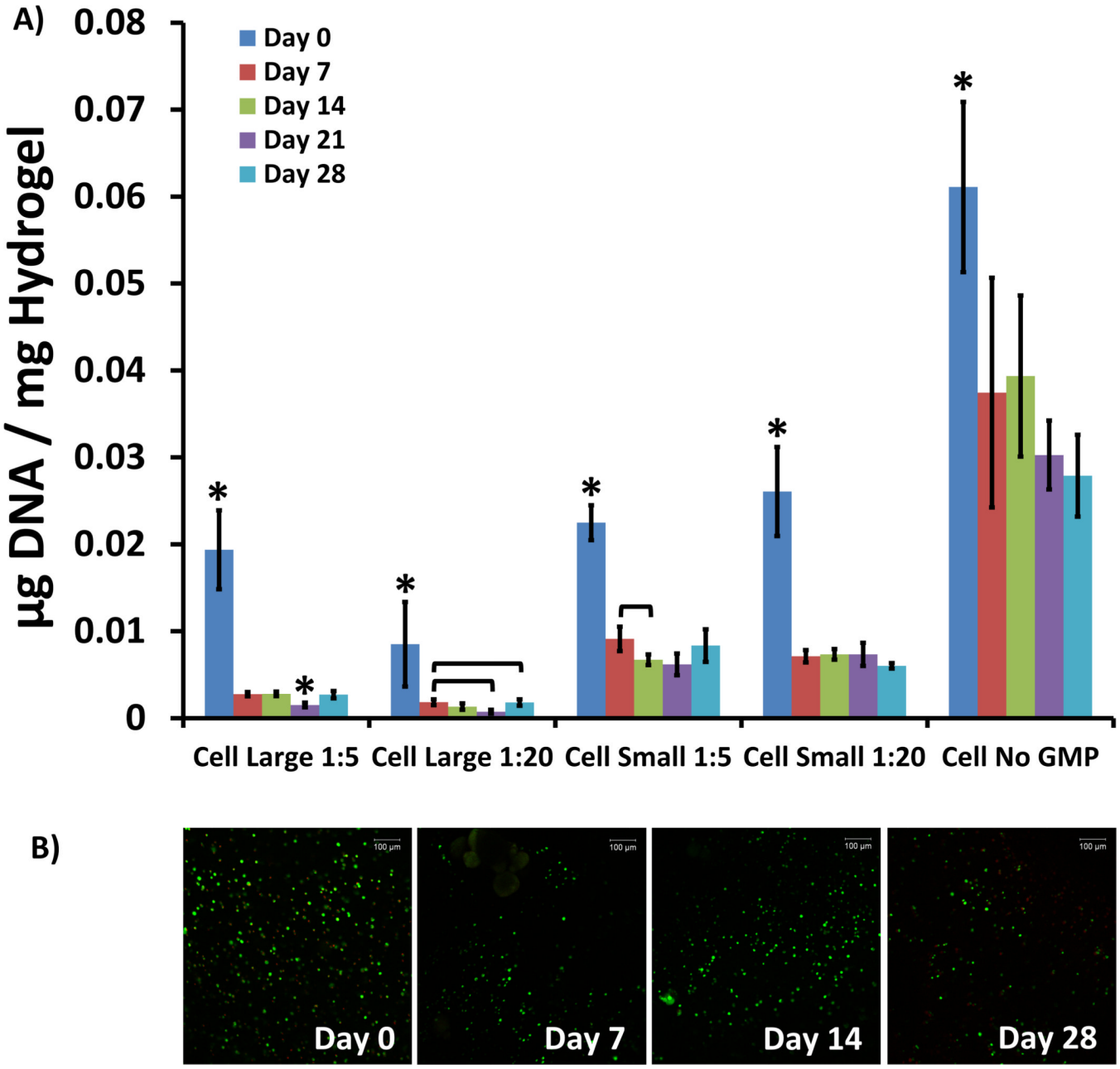

Figure 1.

A) DNA present in cellular hydrogels, expressed as µg DNA / mg Hydrogel, for varying GMP loading and size conditions. Within a group, time-points with * differ from all other time-points ($p < 0.05$). Brackets are used to indicate statistically significant differences between individual time-points within the same condition group ($p < 0.05$). B) Confocal fluorescence microscopy images of Live/Dead-treated sections of cellular hydrogel sections co-encapsulated with 50–100 µm GMPs loaded in a 1:20 ratio. Green staining indicates live cells, and red staining indicates dead cells. Images were taken at 10× original magnification. The scale bar in the upper right corner of each image represents 100 µm.

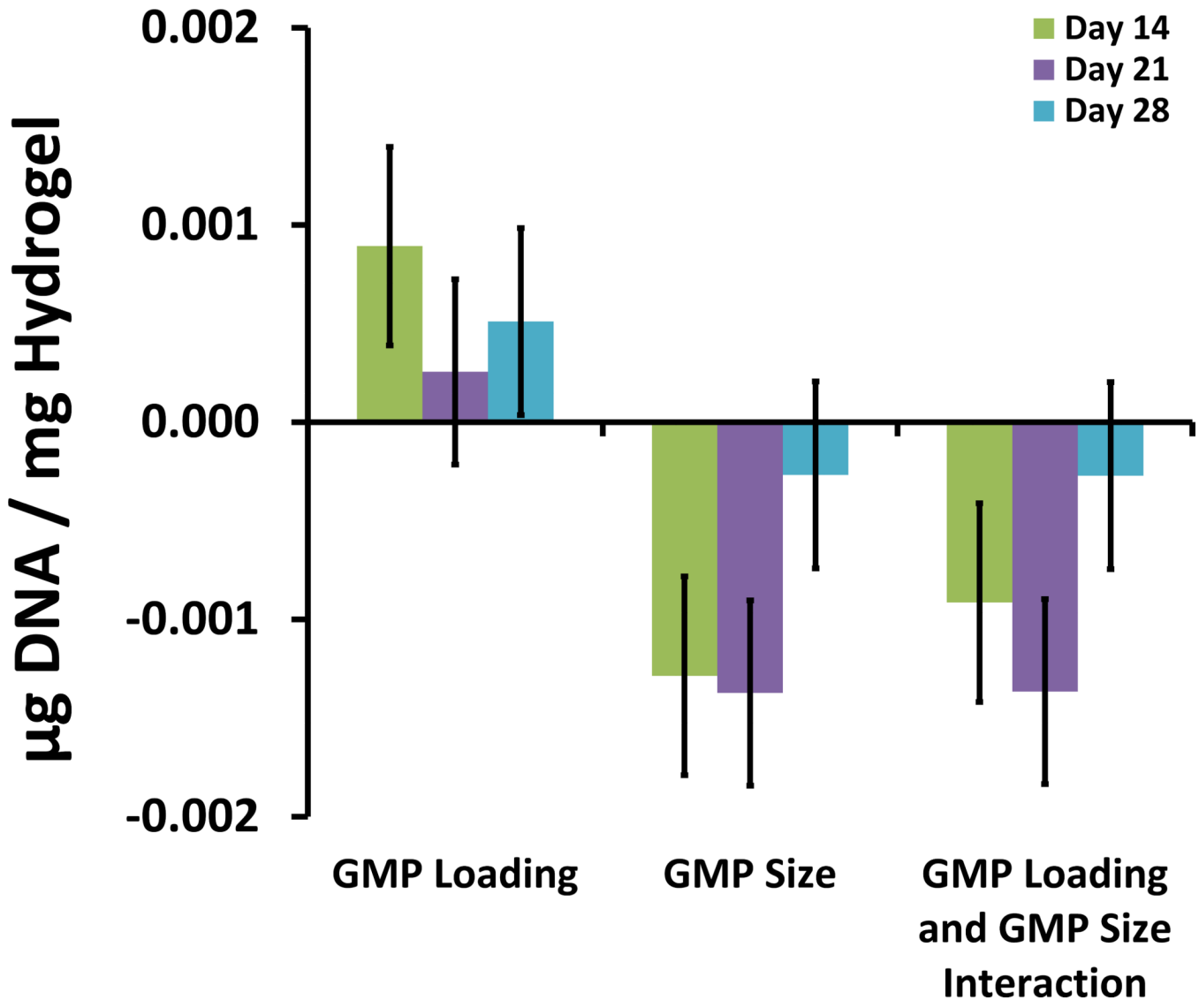

Figure 2.
Main effects and interactions for hydrogel DNA content from full 2^2 factorial analysis at Day 14, 21, and 28. The main effects of GMP loading ratio and GMP size are shown along with the interaction between them.

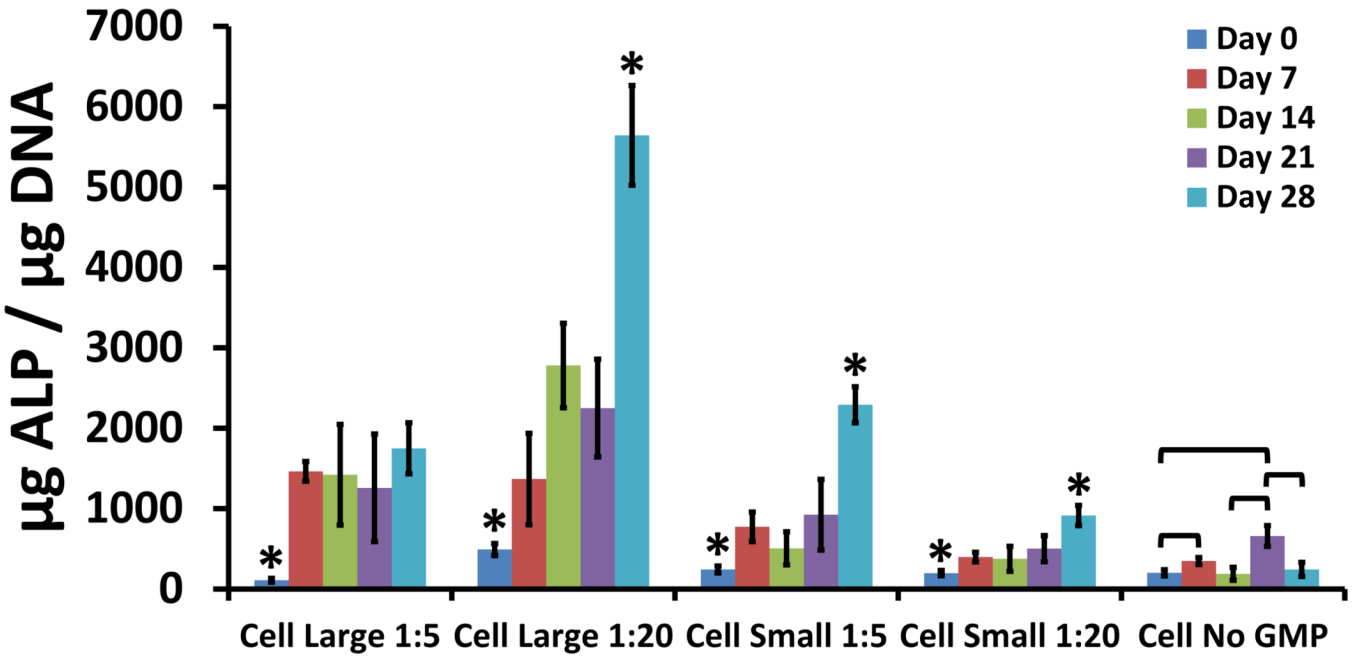

Figure 3.

ALP present in cellular hydrogels, expressed as µg ALP / µg DNA, for varying GMP loading and size conditions. Within a group, time-points with * differ from all other time-points ($p < 0.05$). Brackets are used to indicate statistically significant differences between individual time-points within the same condition group ($p < 0.05$).

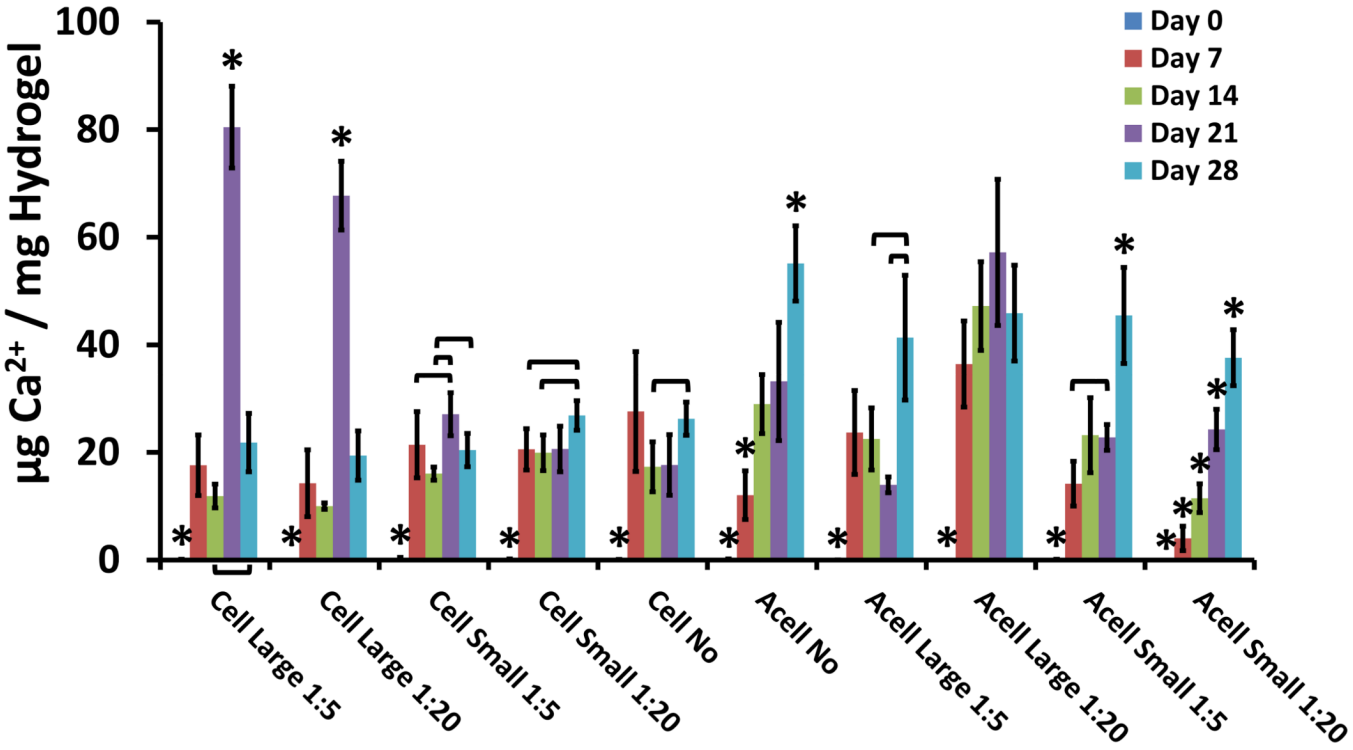

Figure 4.

Calcium present in cellular and acellular hydrogels, expressed as μg Ca^{2+} / mg Hydrogel, for varying GMP loading and size conditions. Within a group, time-points with * differ from all other time-points ($p < 0.05$). Brackets are used to indicate statistically significant differences between individual time-points within the same condition group ($p < 0.05$).

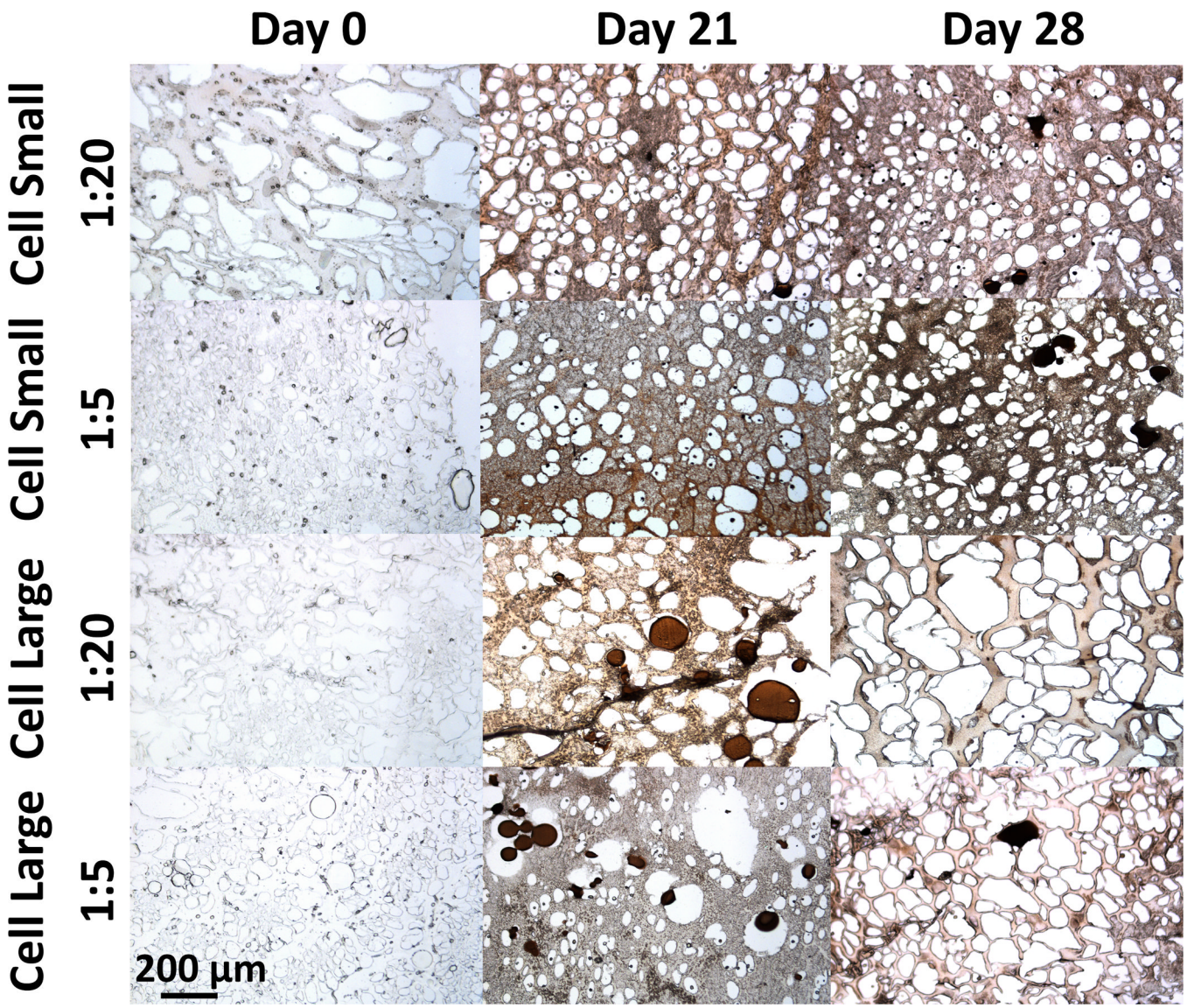

Figure 5.
Hydrogel mineralization for all GMP size and loading conditions as determined by von Kossa staining of 5 µm histological sections 0, 21, and 28 days after encapsulation. Acellular hydrogels are shown for the Day 0 time-point as a control. Images were taken at 100× the original magnification, and the scale bar for 200 µm in the lower left corner applies to all images.

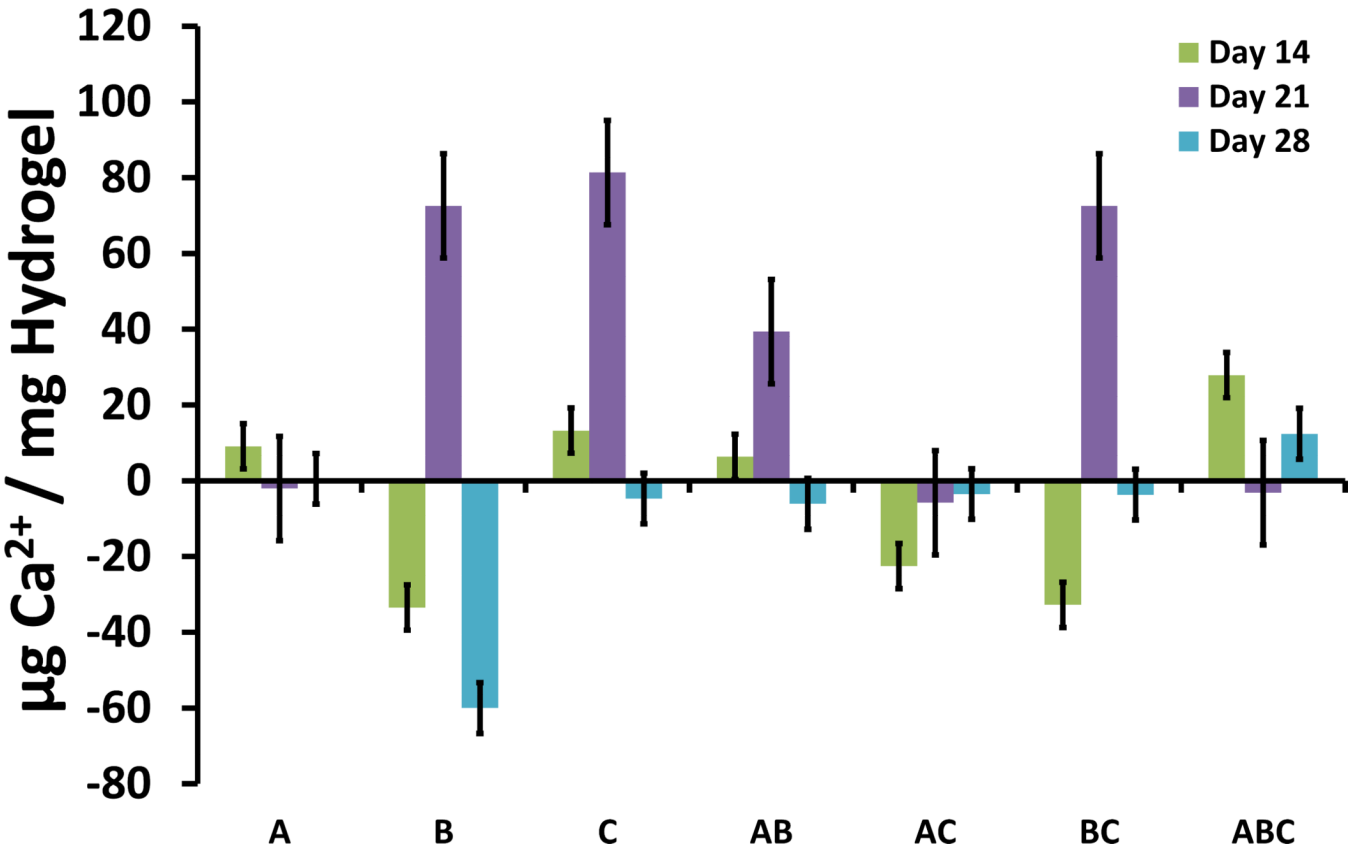

Figure 6.
Main effects and interactions for hydrogel Ca^{2+} content from full 2^3 factorial analysis at Day 14, 21, and 28. The main effects of GMP loading ratio (A), cellularity (B), and GMP size (C) are shown along with the interactions between them.

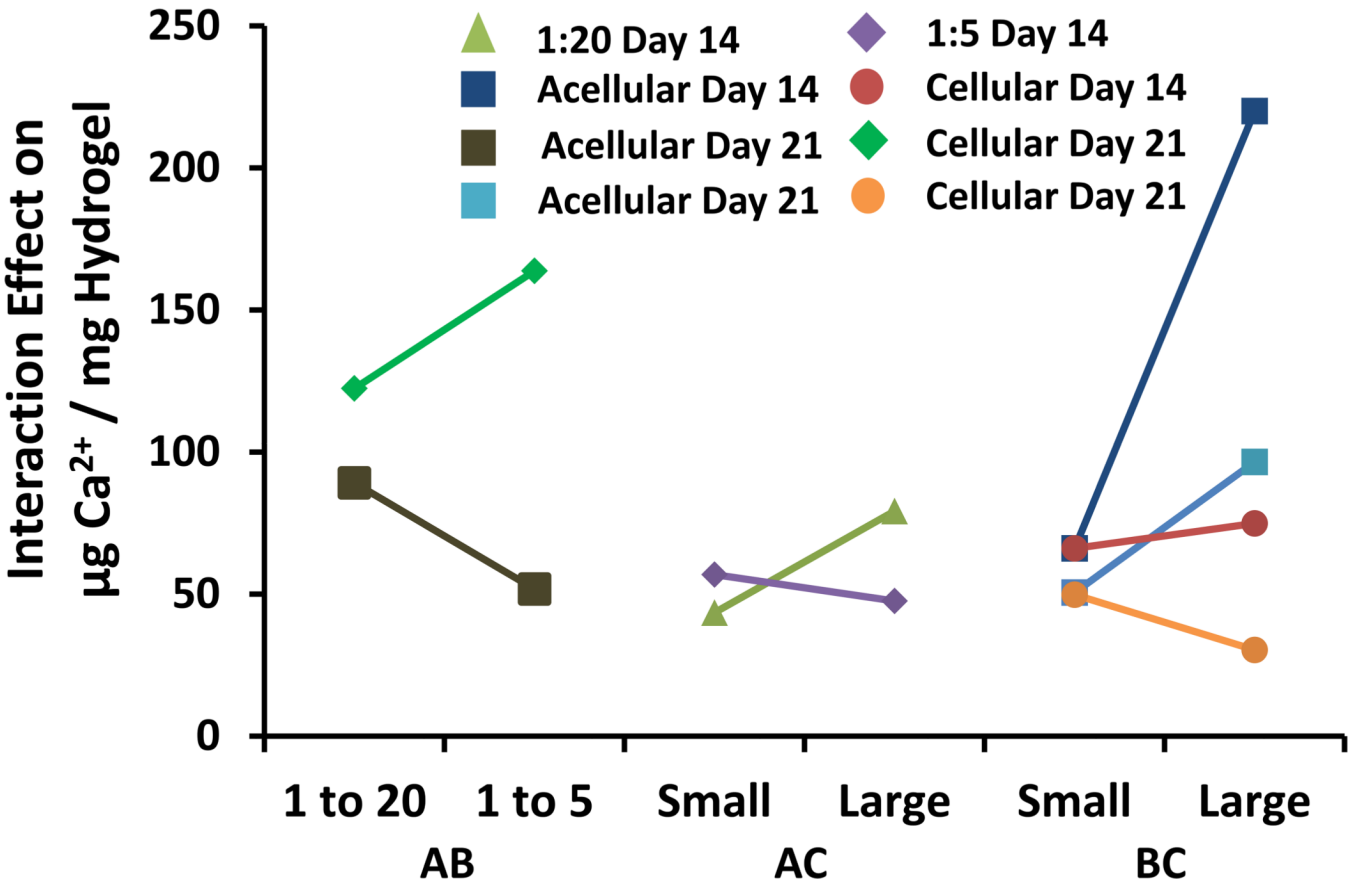

Figure 7.

Interaction effects between GMP size, cellularity, and GMP loading. All curves as labeled are interaction effects from the Day 14 time-point or Day 21 Time-point. The leftmost two curves (AB) represent the interaction effects between GMP size and cellularity. The middle two curves (AC) represent the interaction effects between GMP size and GMP loading. The rightmost four curves (BC) represent the interaction effects between cellularity and GMP loading.

Table 1

Description of study groups for each MSC and GMP loading condition.

Group Name	Cellularity	GMP Size	GMP Loading
Cell Large 1:5	Cellular	250 – 300 μm	1:5
Cell Large 1:20	Cellular	250 – 300 μm	1:20
Cell Small 1:5	Cellular	50 – 100 μm	1:5
Cell Small 1:20	Cellular	50 – 100 μm	1:20
Cell No GMP	Cellular	N/A	None
Acell Large 1:5	Acellular	250 – 300 μm	1:5
Acell Large 1:20	Acellular	250 – 300 μm	1:20
Acell Small 1:5	Acellular	50 – 100 μm	1:5
Acell Small 1:20	Acellular	50 – 100 μm	1:20
Acell No GMP	Acellular	N/A	None